THE JOURNAL OF PHYSICAL CHEMISTRY B

Article

pubs.acs.org/JPCB

Ion Association of Imidazolium Ionic Liquids in Acetonitrile

Marija Bešter-Rogač,*[,†] Alexander Stoppa,[‡] and Richard Buchner*[,‡]

[†]Faculty of Chemistry and Chemical Technology, University of Ljubljana, SI-1000 Ljubljana, Slovenia

[‡]Institut für Physikalische und Theoretische Chemie, Universität Regensburg, D-9304-0 Regensburg, Germany

Supporting Information

ABSTRACT: Molar conductivities, Λ, of dilute solutions of the ionic liquids (ILs) 1-ethyl-3-methylimidazolium tetrafluoroborate ([emim][BF_4]), 1-butyl-3-methylimidazolium tetrafluoroborate ([bmim][BF_4]), 1-butyl-3-methylimidazolium hexafluorophosphate ([bmim][PF_6]), 1-hexyl-3-methylimidazolium tetrafluoroborate ([hmim][BF_4]), and 1-hexyl-3-methylimidazolium bis(trifluoromethanesulfonyl)amide ([hmim][NTf_2]) in acetonitrile (AN) were determined as a function of temperature in the range 273.15−313.15 K. The data were analyzed with Barthel's lcCM model to obtain limiting molar conductivities, $\Lambda^{\infty}(T)$, and association constants, $K_A^{\circ}(T)$ of these electrolytes. The temperature dependence of these parameters, as well as the extracted limiting cation conductivities, λ_i^{∞}, were discussed. Additionally, dielectric spectra for [hmim][NTf_2] + AN were analyzed in terms of ion association and ion solvation and compared with the inference from conductivity. It appears that in dilute solutions the imidazolium ring of the cations is solvated by ∼6 AN molecules that are slowed by a factor of ∼8−10 compared to the bulk-solvent dynamics. Ion association of imidazolium ILs to contact ion pairs is only moderate, similar to common 1:1 electrolytes in this solvent.

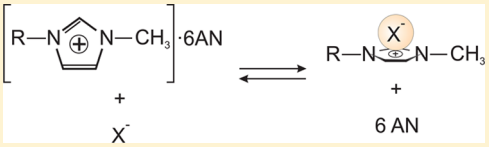

INTRODUCTION

Because of many potential applications[1] room-temperature ionic liquids (ILs), i.e., salts with a melting point around or below room temperature, have been intensively studied for several years now and important information on the properties of this fascinating class of liquids has been accumulated.[2−5] Understanding the properties of pure ILs is of fundamental interest on its own right. However, practical applications generally require the admixture of other compounds, acting either as a reactant or product or as a cosolvent required for process optimization.[6] As the structure and dynamics of IL + solute/cosolvent mixtures vary strongly with composition (see, e.g., refs 7−9 and the dielectric relaxation data for 1-hexyl-3-methylimidazolium bis(trifluoromethanesulfonyl)amide plus acetonitrile ([hmim][NTf_2] + AN) of this contribution), the pure molten salt is not necessarily the optimum reference state for understanding and/or predicting mixture properties.

For binary systems the alternative reference state is the ideal solution, here of the IL in the solvent. Although only hypothetical, as it requires extrapolation of solute properties to infinite dilution, it offers advantages for theory as essentially only solute−solvent and pairwise solute−solute interactions are relevant.[10,11] For 1:1 electrolytes, such as most ILs, the latter reduce to (solvent-mediated) anion−cation interactions that are conveniently expressed by the standard-state association constant

$$K_A^{\circ} = \lim_{c\to 0} K_A(c) = \lim_{c\to 0} \frac{c_{IP}}{c_+ c_-} = \lim_{c\to 0} \frac{1-\alpha}{\alpha^2} \quad (1)$$

where c_{IP}, c_+, and c_- are the molar concentrations of ion pairs, free cations, and free anions at electrolyte concentration c; α is the degree of dissociation, i.e., the fraction of anions (and cations) not bound in ion pairs.[12] Among the various techniques allowing determination of K_A°, thermodynamic methods and dilute-solution conductivity measurements are probably most accurate.[13,14] Their drawback is that they yield—at best—only indirect information on the nature of the aggregate and cannot detect the presence of multistep equilibria involving different solvation states of the ion pair, such as contact (CIPs) and solvent-shared ion pairs (SIPs). On the other hand, dielectric relaxation spectroscopy (DRS) in the microwave region can distinguish various ion-pair species and determine their concentrations as they differ in relaxation time and thus in their position in the dielectric spectrum.[15] However, to do so reliably, reference data for K_A° are needed.[7] Therefore, we recently embarked on a conductivity study of ion association of various imidazolium ILs in a variety of solvents.[16−18] The present contribution is a continuation of that work. We also exemplify the need for such information by presenting a detailed analysis of dielectric spectra of [hmim][NTf_2] + AN mixtures. These data were originally recorded for an investigation of the influence of static relative permittivity, ε, and average dielectric relaxation time of the solvent on the ultrafast transient absorption of a molecular polarity probe but not analyzed in detail then.[19]

EXPERIMENTAL SECTION

Materials and Sample Preparation. The salts 1-ethyl-3-methylimidazolium tetrafluoroborate ([emim][BF_4]), 1-butyl-3-methylimidazolium hexafluorophosphate ([bmim][BF_4]), 1-butyl-3-methylimidazolium hexafluorophosphate ([bmim][PF_6]), and 1-hexyl-3-methylimidazolium bis(trifluoromethanesulfonyl)amide

Received: December 17, 2013
Revised: January 14, 2014

 © XXXX American Chemical Society dx.doi.org/10.1021/jp412344a | J. Phys. Chem. B XXXX, XXX, XXX−XXX

([hmim][BF_4]) were synthesized and purified as described in detail previously;[20] [hmim][NTf_2] was purchased from IoLiTec. Prior to use all compounds were dried at a high-vacuum line ($p < 10^{-8}$ bar) for 7 days at ~313 K, yielding water mass fractions < 50×10^{-6} in Karl Fischer titrations. Potentiometric titration of [bmim][BF_4] samples in aqueous solution against a standard solution of $AgNO_3$ (Carl Roth) yielded <20 × 10^{-6} halide mass fraction. No contaminations were detected with ^{1}H NMR and, where applicable, ^{19}F NMR. The dried ILs were stored in a N_2-filled glovebox. N_2 protection was also maintained when preparing the mixtures and during all subsequent steps of sample handling, including the measurements.

Acetontrile (AN; Merck; Reag. Ph Eur. (Reagent (specification as per) European Pharmacopoeia), >99.9%) was used as received. The conductivity, κ, of the solvent was ~2×10^{-7} $\Omega^{-1}\cdot cm^{-1}$. Stock solutions were prepared by weight from the IL and the solvent.

Conductivity Measurements. Conductivity measurements were carried out as described previously[21] using a three-electrode flow cell in the temperature range of 273.15−313.15 K with ≤0.003 K temperature stability. This involved correction for lead resistance and extrapolation of the conductivities, $\kappa'(\nu)$, recorded in the frequency range of $500 \le \nu/\mathrm{Hz} \le 10000$, to infinite frequency in order to eliminate electrode polarization effects. The corrected conductivities, $\kappa = \lim_{\nu\to\infty} \kappa'(\nu)$, of all investigated systems, converted to molar conductivities, $\Lambda = \kappa/c$, are given in Tables S1 and S2 of the Supporting Information as a function of IL molality, m. The latter relates to the corresponding (temperature-dependent) molarity, c, via $c = m\rho/(1 + M_2 m)$, where M_2 is the molar mass of the solute and ρ the density of the solution. Examples for Λ as a function of $\sqrt{c}$ are shown in Figures 1 and 2. Taking into account all sources of error

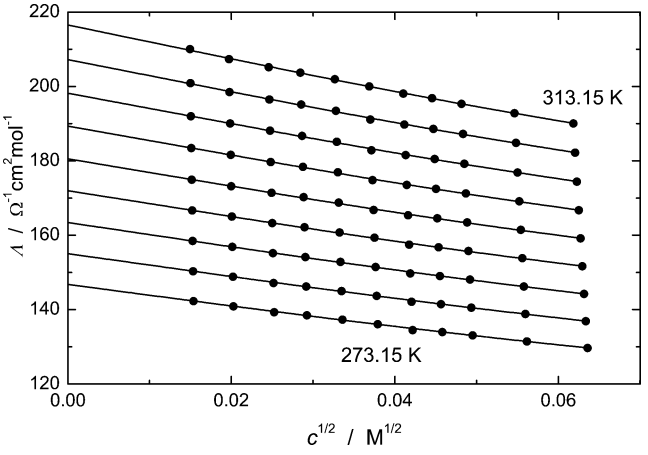

Figure 1. Molar conductivities, Λ (symbols), of [bmim][BF_4] solutions in AN from 273.15 to 318.15 K in steps of 5 K in the concentration range of 0.0005 < c/M < 0.005. Lines show the results of the lcCM fit.

(calibration, measurements, and impurities), the values of κ and Λ are certain within 0.05%.

Density Measurements. Solution densities, ρ, were determined with a vibrating-tube densimeter (Anton Paar DMA 60 and DMA 601 HT) at 298.15 ± 0.02 K and atmospheric pressure. Degassed water and purified nitrogen were used for calibration, assuming densities from standard sources.[22] The precision of the measurements was ±0.1 $kg\cdot m^{-3}$. Considering the possible sources of error (calibration, measurement, and purity of materials), the estimated uncertainty of ρ is within ±0.5 $kg\cdot m^{-3}$.

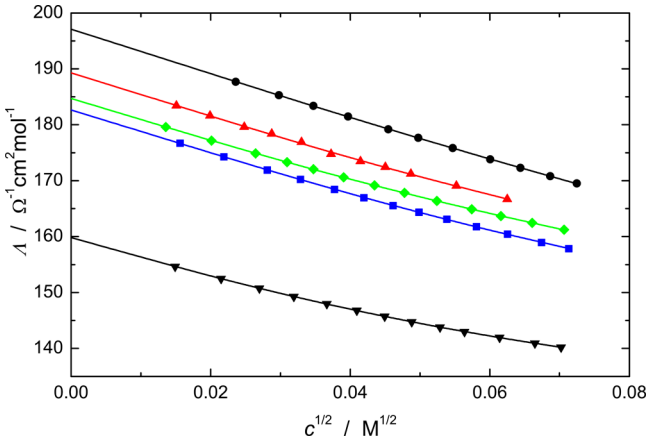

Figure 2. Molar conductivities, Λ (symbols), of ILs in AN at 298.15K: [emim][BF_4] (black filled circles), [bmim][BF_4] (red filled up-triangles), [bmim][PF_6] (green filled diamonds), [hmim][BF_4] (blue filled boxes), and [hmim][NTf_2] (black filled down-triangles); full lines, lcCM fit.

For the investigated dilute solutions ρ increases linearly with increasing salt content,

$$\rho = \rho_s + bm \tag{2}$$

where ρ_s is the density of the solvent taken from the literature[23] (see Table S3 of the Supporting Information for solvent properties), and m is the molality of the IL. The density gradients, b ($kg^2\cdot dm^{-3}\cdot mol^{-1}$), of the studied systems, assumed to be independent of temperature, are included in Tables S1 and S2 of the Supporting Information.

DATA ANALYSIS

Dielectric Spectra. In a previous publication[19] focusing on the effect of static relative permittivity, ε, and average relaxation time, $\langle\tau\rangle$, of the solvent on the ultrafast transient absorption of a molecular polarity probe, we presented dielectric spectra, $\hat{\varepsilon}(\nu) = \varepsilon'(\nu) - i\varepsilon''(\nu)$ (Figure 1 of ref 19; $\varepsilon'(\nu)$ is the relative permittivity and $\varepsilon''(\nu)$ the dielectric loss), of [hmim][NTf_2] + AN mixtures at 298.15 K, covering the entire mixture range at $0.2 \le \nu/\mathrm{GHz} \le 89$. As the quantities of interest then, $\varepsilon = \lim_{\nu\to 0}\varepsilon'(\nu)$ and $\langle\tau\rangle = (2\pi\nu_{pk})^{-1}$ (ν_{pk} is the frequency of the maximum of $\varepsilon''(\nu)$), could be easily extracted from the spectra, we abstained from a formal fit of $\hat{\varepsilon}(\nu)$ and its detailed interpretation. This should be made up in this contribution as the results support recent investigations on IL + AN mixtures[7,24,25] but also show the need of DRS for reliable benchmark data for K_A°, determined by an alternative method such as dilute-solution conductivity measurements.

Details of the DRS measurements were given by Lohse et al.,[19] and information on the fitting procedure and the selection criteria for the choice of the best relaxation model can be found elsewhere.[7,25,26] It may therefore suffice to give the outcome: All mixture spectra, as well as that of neat [hmim][NTf_2], were best described by the equation

$$\hat{\varepsilon}(\nu) = \frac{S_1}{1 + (i2\pi\nu\tau_1)^{1-\alpha_1}} + \frac{S_2}{1 + i2\pi\nu\tau_2} + \varepsilon_\infty \tag{3}$$

Equation 3 is the superposition of a lower frequency Cole−Cole (CC) equation (mode 1), of amplitude S_1, relaxation time τ_1, and width parameter α_1, with a higher frequency Debye (D) mode (2), of amplitude S_2 and relaxation time τ_2. The infinite-frequency permittivity, $\varepsilon_\infty = \lim_{\nu\to\infty}\varepsilon'(\nu)$, accounts for

dx.doi.org/10.1021/jp412344a | J. Phys. Chem. B XXXX, XXX, XXX−XXX

intramolecular polarizability. All obtained fit parameters, together with the value of the reduced error function of the fit, χ_r^2,[26] the density, ρ, and electrical conductivity, κ, of the studied mixtures are tabulated as a function of IL mole fraction, x, in Table S4 of the Supporting Information. Examples of the spectra and their fits are given in Figure S1 of the Supporting Information.

As detailed in ref 7, dielectric amplitudes, S_j (j = 1, 2), were evaluated with the Cavell equation

$$\frac{2\varepsilon + 1}{\varepsilon} S_j = \frac{N_A}{k_B T \varepsilon_0} c_j \mu_{\mathrm{eff},j}^{\ 2} \tag{4}$$

assuming spherical cavity and reaction fields. Equation 4 relates S_j of process j to molar concentration, c_j, and effective dipole moment, $\mu_{\mathrm{eff},j}$, of the species responsible for that process. The latter incorporates induced contributions to dipole−dipole interactions in the liquid via the apparent moment $\mu_{\mathrm{ap},j} = \mu_j/(1-f_j\alpha_j)$, where μ_j is the gas-phase moment, f_j the reaction field factor, and α_j the polarizability of the dipole. Additionally, possible orientational correlations of the dipoles are taken into account by an empirical correlation factor, g_j, with $\mu_{\mathrm{eff},j} = \mu_{\mathrm{ap},j}(g_j)^{1/2}$.[27]

Conductivity. The obtained molar conductivities, $\Lambda(c)$ (Tables S1 and S2 of the Supporting Information and Figures 1 and 2), of dilute ($\lesssim$0.005 M) IL solutions were analyzed in the framework of Barthel's low-concentration chemical model (lcCM).[10] For the evaluation of Λ this approach uses the equation

$$\frac{\Lambda}{\alpha} = \Lambda^\infty - S\sqrt{\alpha c} + E\alpha c \ln(\alpha c) + J_1 \alpha c - J_2 (\alpha c)^{3/2} \tag{5}$$

where

$$K_A^\circ = \frac{1-\alpha}{\alpha^2 c (y_\pm')^2}; \qquad y_\pm' = \exp\left(-\frac{\kappa_D q}{1+\kappa_D R_{ij}}\right) \tag{6}$$

$$\kappa_D^{\ 2} = 16\pi N_A q \alpha c; \qquad q = \frac{e^2}{8\pi\varepsilon_0 \varepsilon k_B T} \tag{7}$$

In eqs 5−7, Λ^∞ is the molar conductivity at infinite dilution, $(1-\alpha)$ the fraction of oppositely charged ions bound in ion pairs, and K_A° the standard-state (infinite dilution) ion association constant. The activity coefficients of the free cations, y_+', and anions, y_-', define $(y_\pm')^2 = y_+' y_-'$, while κ_D is the Debye parameter, e is the proton charge, ε is the static relative permittivity of the solvent, T is the Kelvin temperature, and k_B and N_A are the Boltzmann and Avogadro constants, respectively. Expressions for the coefficients S, E, J_1, and J_2 of eq 5 can be found in ref 10. The limiting slope, S, and the parameter E are fully defined by the known[23] values for density, ρ_s, viscosity, η, and static relative permittivity, ε, of neat AN (Table S3 of the Supporting Information). The coefficients J_1 and J_2 are functions of the distance parameter, R_{ij}.

The lcCM model counts two oppositely charged ions as an ion pair if their mutual separation, r, is within the limits $a \le r \le R_{ij}$, where $a = r_+ + r_-$ is the distance of closest approach of cation and anion and R_{ij} represents the distance up to which oppositely charged ions can approach as independently moving particles in the solution. As there are good indications from quantum-chemical calculations[28] and simulations[29] that BF_4^- and PF_6^- are preferably located above the imidazolium ring of the cation, the same effective cation radius, r_+ = 0.133 nm,[30] was chosen for $[emim]^+$, $[bmim]^+$, and $[hmim]^+$. As anion radius r_- = 0.232 nm was taken for BF_4^-,[23] and that of 0.370 nm for PF_6^-,[23] based on semiempirical calculations,[31] r_- = 0.35 nm was selected for $[NTf_2]^-$. Assuming the possible existence of contact (CIP) and solvent-shared (SIP) ion pairs, the upper integration limit was taken as $R_{ij} = a + s$, where s = 0.58 nm is the length of an oriented AN molecule.[23]

Data analysis was carried out by a nonlinear least-squares fit, with coefficients S, E, and J_1 of eq 5 preset to their calculated values and with Λ^∞, K_A°, and J_2 as the adjustable parameters.[10,23] The thus obtained results for Λ^∞ and K_A° are summarized in Table 1. Also included are the distance parameters $R_{ij}(J_2)$ calculated from the adjusted J_2 values, which are in good agreement with the assumed values, R_{ij}, indicating self-consistency of the fits.[10]

Table 1. Limiting Molar Conductivities, Λ^∞, Association Constants, K_A°, and Values for the Parameter $R_{ij}(J_2)$ for Solutions of Imidazolium ILs in AN[a]

T	Λ^∞	K_A°	$R_{ij}(J_2)$	Λ^∞	K_A°	$R_{ij}(J_2)$
		[emim][BF_4]			[bmim][BF_4]	
273.15	152.84	13.7	0.979	146.78	14.1	0.802
278.15	161.47	14.3	0.965	155.05	14.1	0.828
283.15	170.20	14.2	0.992	163.41	14.4	0.823
288.15	179.06	15.5	0.942	171.96	15.2	0.786
293.15	188.02	15.5	0.961	180.50	15.5	0.773
298.15	197.10	15.9	0.959	189.29	15.7	0.796
303.15	206.30	16.4	0.953	198.17	16.1	0.795
308.15	215.65	17.0	0.947	207.18	16.6	0.779
313.15	225.12	17.4	0.945	216.52	17.2	0.802
		[bmim][PF_6]			[hmim][BF_4]	
273.15	143.25	14.6	0.907	141.55	15.3	0.746
278.15	151.31	14.6	0.914	149.53	15.4	0.753
283.15	159.49	14.8	0.917	157.64	15.5	0.751
288.15	167.79	15.1	0.916	165.85	15.7	0.757
293.15	176.18	15.3	0.919	174.16	15.6	0.805
298.15	184.70	15.6	0.919	182.65	16.5	0.757
303.15	193.36	15.8	0.924	191.21	16.7	0.769
308.15	202.09	15.9	0.933	199.90	17.1	0.767
313.15	210.97	16.1	0.945	208.71	17.3	0.780
		[hmim][NTf_2]				
273.15	123.68	12.05	0.728			
278.15	130.69	12.10	0.735			
283.15	137.80	12.13	0.741			
288.15	145.03	12.23	0.747			
293.15	152.39	12.64	0.735			
298.15	159.82	12.67	0.741			
303.15	167.38	12.76	0.750			
308.15	175.08	13.15	0.742			
313.15	182.90	13.41	0.742			

[a]The assumed upper limit of association is R_{ij} = 0.945 nm for the tetrafluoroborates, 1.083 nm for [bmim][PF_6], and 1.063 nm for [hmim][NTf_2]. Units: T, K; Λ^∞, $\Omega^{-1}\cdot cm^2\cdot mol^{-1}$; K_A°, M^{-1}; $R_{ij}(J_2)$, nm.

RESULTS AND DISCUSSION

Dielectric Relaxation. The dielectric spectra of [hmim][NTf_2] + AN (Figure S1 of the Supporting Information) strongly resemble those of previously investigated imidazolium IL + AN mixtures and accordingly can be formally described by the sum of a lower frequency Cole−Cole equation (mode 1) at ~1−3 GHz and a Debye equation peaking at $\gtrsim$20 GHz (mode 2).[7] Qualitatively, this similarity also extends to the composition dependence of the obtained amplitudes, S_j (j = 1, 2; Figure 3),

dx.doi.org/10.1021/jp412344a | J. Phys. Chem. B XXXX, XXX, XXX−XXX

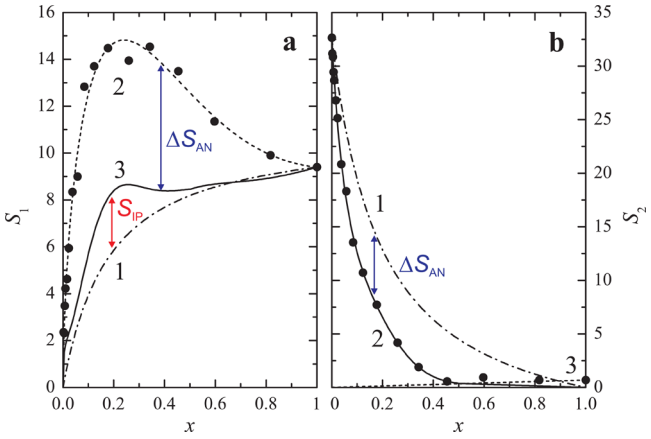

Figure 3. Amplitudes (black filled circles) of (a) the lower frequency CC mode, S_1, and (b) the higher frequency D mode, S_2, of [hmim][NTf_2] + AN mixtures at 298.15 K. In panel a curve 1 is the amplitude expected from the effective dipole moment of $[hmim]^+$ and the analytical IL concentration, curve 2 is an empirical fit of the experimental data, and curve 3 is the IL-related component of S_1 (see text for details). In panel b curve 1 shows the amplitude expected for AN and curve 2 an empirical fit of S_2, corrected for the contribution from IL cage rattling, curve 3.

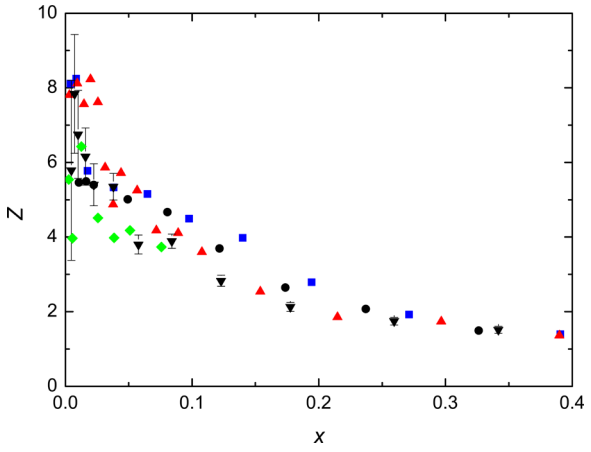

Figure 4. Solvation numbers, Z (black filled down-triangles), of [hmim][NTf_2] in AN at 298.15 K. Also included are the data of Stoppa et al.[7] for [emim][BF_4] (black filled circles), [bmim][BF_4] (red filled up-triangles), and [hmim][BF_4] (blue filled boxes), as well as of Bešter et al.[18] for [bmim][Cl] (green filled diamonds). Error bars, which are similar for all ILs, correspond to the standard deviation of a low-order polynomial fit to S_2.

relaxation times, τ_j (Figure S2 of the Supporting Information), and the CC width parameter, α_1 (Figure S3 of the Supporting Information). In analogy to ref 7, we may therefore assign mode 2 to the reorientation of free AN molecules, which predominates at low IL mole fraction but apparently dies out at $x \approx 0.5$, plus a small contribution from cage-rattling modes of [hmim][NTf_2]. Similarly, mode 1 is a superposition of contributions from cation and ion-pair reorientation, as well as from weakly bound AN.

Solvation. At low IL content the amplitude of the higher frequency mode rapidly drops from the pure-AN value, S_2 = 32.63, to ~0.6 at x = 0.45 and then remains essentially constant (Figure 3b, symbols). Except for the pure IL, S_2 is always smaller than expected from the analytical AN concentration (Figure 3b, curve 1, calculated with eq 4 under the assumption that AN molecules in the mixtures have the same effective dipole moment as in neat AN, $\mu_{eff,AN}$ = 4.34 D[7]). This implies that part of the solvent interacts so strongly with [hmim][NTf_2] that its dynamics is notably different from that of "free" AN. As a result, the corresponding amplitude, ΔS_{AN}, is missing from the solvent contribution.

The amount of bound AN was calculated from the analytical, c_{AN}, and the apparent, i.e., DRS-detected, solvent concentration, c_{AN}^{ap}. The latter was obtained with eq 4 from S_2 after correction for the small contribution from IL cage rattling, which was assumed to be proportional to x (Figure 3b, curve 3). Normalization to the IL concentration, c, yielded the effective solvation number

$$Z = (c_{AN} - c_{AN}^{ap})/c \quad (8)$$

shown in Figure 4.

The obtained $Z(x)$ values, Figure 4, smoothly decrease from ~6–7 at $x \to 0$ to $Z = 0$ at $x = 1$, possibly with two linear branches and a breakpoint at $x \approx 0.2$. At $x \gtrsim 0.5$ the effective solvation number approaches the molar AN:IL ratio, so that no "free" acetonitrile is present anymore. Over the entire composition range the effective solvation numbers for [hmim][NTf_2] in AN agree with those published for [emim][BF_4], [bmim][BF_4], and [hmim][BF_4],[7] as well as for [bmim][Cl][18] (Figure 4). In other words, for all imidazolium ILs investigated so far, the effective solvation number obtained with DRS does neither depend on the anion nor on the length of the cation's alkyl chain. The lacking anion effect can be easily understood from the small donor number of AN, making it a typical aprotic protophobic solvent with poor anion solvation.[10] The obtained Z values may thus be assigned to the cations. The lacking dependence on side-chain length suggests that the bound AN molecules are only interacting with the imidazolium ring, which is solvated by ~6–7 AN molecules at infinite dilution. This is in line with a recent study of Bardak et al.,[24] combining MD simulation and OKE spectroscopy, who found AN–cation complexes in [C_5mim][NTf_2] + AN. Also, based on infrared spectroscopy, Zheng et al.[32] claim that two types of interactions are responsible for cation solvation in these systems: hydrogen bonding between the nitrogen atom of AN molecules and the three hydrogen atoms of the imidazolium moiety, as well as the dispersive attraction exerted by the aromatic ring on the methyl groups of the AN molecules sitting above and below the ring (probably strengthened by ion-dipole forces). However, both kinds of cation–AN interactions cannot be much stronger than AN–AN and ion–ion interactions in these mixtures. This is suggested by the marked decrease of Z with increasing IL concentration, an effect commonly explained by competing ion–ion-solvent interactions and solvation-shell overlap.[15] Additionally, as for all previously investigated imidazolium IL + AN mixtures[7,18] but in contrast to ethylammonium nitrate + AN,[25] also for [hmim][NTf_2], these bound solvent molecules are not completely frozen in their dynamics but only slowed down by a factor of ~8–10 (Figure S2 of the Supporting Information) as they (probably accidentally) contribute to the lower frequency mode 1; see subsequent text.

Ion-Pair and Cation Relaxation. With increasing mole fraction the amplitude of the IL-related lower frequency mode steeply rises from S_1 = 0 to a pronounced maximum of $S_1 \approx 14.5$ at $x \approx 0.25$, coinciding with the minimum in the excess volume of the mixtures (Figure S4 of the Supporting Information), before decreasing to the pure-IL value of 9.40 (Figure 3a, symbols). Clearly, for all mixtures the experimental amplitude is larger than that expected for $[bmim]^+$ (Figure 3a, curve 1) if it is assumed that the IL cation were the only dipolar species contributing to mode 1. The latter was calculated with eq 4 from the analytical IL concentration assuming for all x the effective cation dipole moment of $\mu_{eff,IL}$ = 5.88 D derived from S_1 of pure [hmim][NTf_2].

dx.doi.org/10.1021/jp412344a | J. Phys. Chem. B XXXX, XXX, XXX–XXX

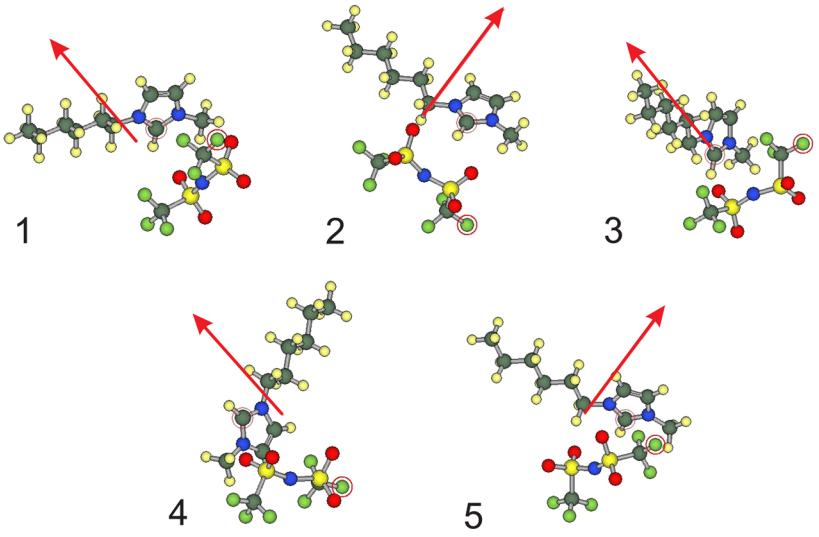

Figure 5. Most stable CIP conformations for [hmim][NTf_2] in AN obtained from semiempirical calculations using MOPAC2009[31] with the PM6 Hamiltonian and COSMO. Their heats of formation (kJ·mol^{-1}) and $\mu_{IP,eff}$/D are as follows: (1) −2056 and 19.9; (2) −2056 and 20.2; (3) −2047 and 24.7; (4) −2046 and 26.7; (5) −2043 and 25.4. The arrows indicate the direction of the dipole moment.

As in previous investigations of similar systems,[7,18] the concentration dependence of ε (Figure 3 of ref 19), the relaxation time of mode 1, τ_1 (Figure S2 of the Supporting Information), and especially the effective dipole moment, $\mu_{IL,eff}$, calculated from S_1 (Figure S5 of the Supporting Information) suggest the presence of ion pairs in [hmim][NTf_2] + AN mixtures. However, not the entire difference between expected and experimentally determined S_1 values can be due to ion-pair relaxation as this would require an unrealistically high association constant (∼500 M^{-1}). Following the arguments in refs 7 and 18, it is therefore assumed that the bound AN molecules contribute to mode 1. Accordingly the present S_1 (for convenience fitted to a polynomial, curve 3 in Figure 3a) were corrected for the lacking AN amplitude, ΔS_{AN}, of Figure 3b. From the resulting curve 3 of Figure 3a $\mu_{IL,eff}$ was calculated with eq 4. Similar to previous mixture studies,[7,18,33,34] the effective dipole moment of the IL stays at the value of the pure IL, 5.88 D, down to $x \approx 0.4$ before increasing first gradually on further dilution[35] and then shooting off at $x \lesssim 0.05$. It extrapolates to $\mu_{IL,eff}(x{=}0) \approx 17$ D (Supporting Information Figure S5).

The effective moment of pure [hmim][NTf_2], 5.88 D, is somewhat larger than the value for [hmim][BF_4], 4.6 D.[36] This suggests some contribution from $[NTf_2]^-$ for which MOPAC[31] yields μ_{eff} = 5.3 D for its cis and 0.5 D for its trans conformer. Indeed, assuming additivity of anion and cation amplitudes and inserting the effective dipole moment of [hmim][BF_4] as the cation value into eq 4 ($[BF_4]^-$ has no permanent dipole moment) yields for the anion $\mu_{-,eff}$ = 3.7 D, which corresponds to 49% cis conformer in the pure IL. This result is in excellent agreement with the simulations and Raman data of Canongia Lopes et al.[37] who found 48% cis at room temperature. On the other hand, as expected from the only moderate tendency of imidazolium ILs to associate in AN,[7,38] the $x \to 0$ value for the effective dipole moment of [hmim][NTf_2] is significantly smaller than that predicted for possible ion pairs.[39] Here MOPAC yielded values of $\mu_{CIP,eff}$ = 19.6−26.7 D for the most stable conformations of the contact ion pair (CIPs, Figure 5). For SIPs, which are unlikely because of the unstable cation solvation shell,[7] even larger values (∼40 D) would be expected.

In principle, α, and thus c_{IP}, is readily accessible[7] from $\mu_{IL,eff}(x)$ at any x as for the considered one-step equilibrium

$$\alpha(x) = \frac{\mu_{IP,eff}^{\ 2} - \mu_{IL,eff}^{\ 2}(x)}{\mu_{CIP,eff}^{\ 2} - \mu_{IL,eff}^{\ 2}(x=1)} \tag{9}$$

However, this requires a reliable value for $\mu_{IP,eff}$ as input into eq 9 because the resulting ion-pair concentrations and the corresponding association constants are strongly affected by the choice of the ion-pair dipole moment. This is clearly seen in Supporting Information Figure S6 and Figure 6, which show c_{IP}

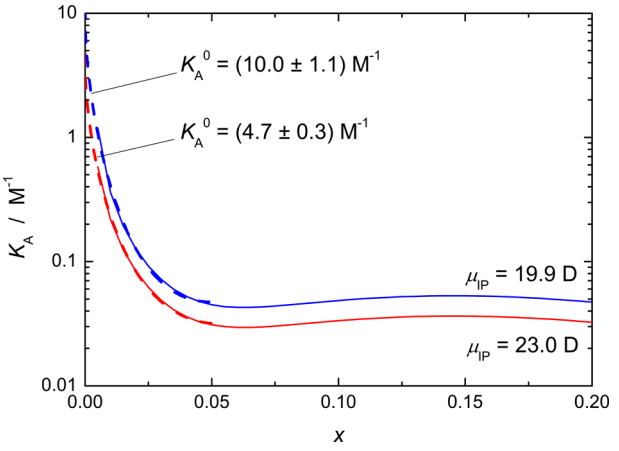

Figure 6. Association constants, $K_A(x)$ (solid lines), of [hmim][NTf_2] + AN mixtures at 298.15 K calculated from curve 3 of Figure 3 for the average (23 D) and the smallest (19.9 D) effective dipole moment of the five most stable ion-pair conformations (Figure 5). Also shown are the corresponding Guggenheim-type fits (broken lines) used to extrapolate $K_A(x)$ to K_A°.

and $K_A(x)$ values, respectively, calculated for the average (23 D) and the smallest (19.6 D) dipole moment of the five minimum-energy conformations found for CIP, Figure 5. As a consequence, the resulting K_A° = 4.7 and 11.0 M^{-1}, respectively, obtained from extrapolating $K_A(x)$ to infinite dilution with a Guggenheim-type equation,[7] also differ significantly. This shows that in principle

dx.doi.org/10.1021/jp412344a | J. Phys. Chem. B XXXX, XXX, XXX−XXX

DR studies can yield the most probable ion-pair species. However, to do so additional information from other methods, such as for instance benchmark values for K_A°, is required. This is especially the case for the present example, [hmim][NTf_2] + AN, where the ion-pair relaxation could not be resolved as a separate mode in the spectra and thus the corresponding relaxation time, which informs on the ion-pair size, is not available.

CONDUCTIVITY STUDIES

As a spectroscopic technique monitoring—at least in principle—the individual contributions of all dipolar species DRS provides molecular-level information over the entire mixture range of binary IL + polar solvent systems. This was exemplified in the preceding section, which also showed that supplementary information from other techniques is required to interpret the dielectric data. In parallel, also the conductivity of all studied [hmim][NTf_2] + AN mixtures was determined (Supporting Information Table S4). Such data are relevant for practical applications and accordingly in the focus of many studies; see, e.g., refs 6, 20, 38, and 40. However, for concentrated solutions $\Lambda(x)$ is notoriously difficult to interpret as changing viscosity superimposes the effects arising from ion association to pairs, triples, and possibly larger aggregates. As a result the variation of $\Lambda(x)$ is generally rather unspecific when going from dilute solutions to the pure IL (Supporting Information Figure S4). Accordingly, we abstain from discussing the conductivity data of concentrated [hmim][NTf_2] solutions summarized in Supporting Information Table S4 and Figure S4. On the other hand, for dilute solutions ($c \lesssim 10^{-2}$ M) only ion pairing is relevant. Here the theory for evaluating the concentration dependence of Λ in terms of the electrolyte's limiting molar conductivity, Λ^∞, and K_A° is well established and accurate information can be obtained.[10,11] Although also this technique has its problems for $K_A^\circ \lesssim 10$ M^{-1}, it is safe to say that among all available methods dilute-solution conductivity measurements yield the most reliable association constants of binary symmetrical electrolytes.[13,14]

Ion Association. Standard-state association constants were determined with dilute-solution ($c \lesssim 0.005$ M) conductivity measurements for a series of imidazolium IL solutions in AN (Table 1) to provide benchmark data for cation−anion interactions in these systems. For [hmim][NTf_2] + AN $K_A^\circ = 12.67$ M^{-1} was found for 298.15 K. This value is in good agreement with the DRS result (10.0 ± 1.1 M^{-1}) for the smallest CIP dipole moment, suggesting that conformer 1 of Figure 5, where the $[NTf_2]^-$ anion in cis conformation is on top of the imidazolium ring, is the predominating ion-pair species in these solutions. Such a configuration is compatible with the findings of Zheng et al.[32] for [bmim][BF_4] + AN. However, this good agreement between dielectric and conductivity result should be taken with a grain of salt as up to now the minimum concentration for which the solute relaxation of 1:1 electrolytes can be resolved with DRS is ~0.05 M. From here, extrapolation of $K_A(x)$ to infinite dilution is still far and the DRS-detected K_A° thus very sensitive to experimental errors. Nevertheless, identification of the ion-pair species, i.e., distinction between CIP and SIP (and 2SIP[15]), should always be possible by comparing the DRS result with benchmark K_A° from dilute-solution conductivity measurements.

The outcome of dilute-solution conductivity measurements, K_A°, and Λ^∞, are not only useful as benchmarks in the evaluation of data obtained with other techniques. Especially, the temperature dependence of these quantities is a valuable source of information itself; see subsequent discussion. Already a comparison of the present standard-state association constants (Table 1) with such data for "conventional" 1:1 electrolytes is revealing: The present imidazolium ILs have very similar K_A° values in the range of only 12−17 M^{-1}. Ion association of these compounds in AN is thus rather weak and comparable to sodium tetraphenylborate (K_A° = 13.9 M^{-1} at 298.15 K).[41] This is in marked contrast to ethylammonium nitrate where $K_A^\circ \approx 1000$ M^{-1} in AN because of the hydrogen bond stabilizing the CIP.[25] But even alkali metal and tetraalkylammonium salts generally exhibit somewhat stronger ion pairing in this solvent (K_A° = 20−50 M^{-1}).[23,41] Almost certainly the rather weak ion pairing of imidazolium ILs in AN is due to the low surface-charge density of their ions. The present K_A° (and Λ^∞) of the tetrafluoroborates, Table 1, are in reasonable agreement with those obtained by Kalugin et al.[38] but differ considerably from those of Wang et al.[42] who reported association constants of ~700 M^{-1} for [bmim][BF_4] and [bmim][PF_6]. Their Λ^∞ values are also markedly smaller.[42]

From K_A° the standard Gibbs energy of association, ΔG_A°, was obtained as

$$\Delta G_A^\circ = \Delta H_A^\circ - T\Delta S_A^\circ = -RT \ln K_A^\circ \quad (10)$$

Figure 7 summarizes the present results: For all investigated imidazolium ILs ΔG_A° is negative and decreases with increasing T.

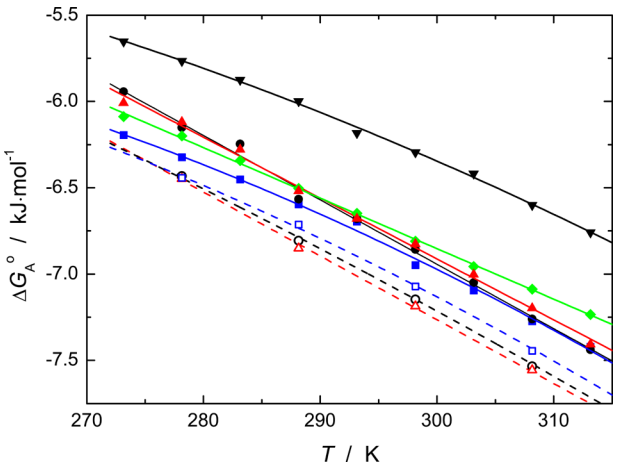

Figure 7. Gibbs energy of ion association, ΔG_A°, as a function of T, for ILs in AN: [emim][BF_4] (black filled circles), [bmim][BF_4] (red filled up-triangles), [bmim][PF_6] (green filled diamonds), [hmim][BF_4] (blue filled boxes), and [hmim][NTf_2] (black filled down-triangles). Lines are calculated with eq 11 and parameters of Table 2. Open symbols and broken lines show corresponding tetrafluoroborate data of Kalugin et al.[38]

Except for [hmim][NTf_2] the K_A° and thus ΔG_A° values are very similar but the slope for [bmim][PF_6] differs notably from that of the tetrafluoroborates, whereas the data for both [hmim] ILs show a marked curvature. Also included in Figure 7 are the results of Kalugin et al.[36] for the tetrafluoroborate ILs. For all cations they studied, ΔG_A° is somewhat lower than the present data. Besides small differences in the experimental conductivity data, this is mainly due to the different conductance equation used in ref 38. However, both data sets are essentially parallel, yielding thus the same message regarding the driving force for ion association of imidazolium ILs in AN; see subsequent discussion.

Using the common thermodynamic relationships, the temperature dependence of ΔG_A° can be expressed as

$$\Delta G_A^\circ(T) = \Delta H_{A,298}^\circ + \Delta C_{pA}(T - T^*) - T[\Delta S_{A,298}^\circ + \Delta C_{pA} \ln(T/T^*)] \quad (11)$$

dx.doi.org/10.1021/jp412344a | J. Phys. Chem. B XXXX, XXX, XXX−XXX

Table 2. Standard Free Energy, $\Delta G^{\circ}_{A,298}$,[a] Standard Enthalpy, $\Delta H^{\circ}_{A,298}$[a], Standard Entropy, $\Delta S^{\circ}_{A,298}$, and Heat Capacity Change, ΔC_{pA}, of Ion Association at 298.15 K with Eyring Activation Enthalpy of Charge Transport, $\Delta H^{\ddagger}(\Lambda)$, for Ionic Liquids in Various Solvents of Static Permittivity, ε, and Activation Enthalpy of Viscous Flow, $\Delta H^{\ddagger}(\eta)$[b]

IL	$\Delta G^{\circ}_{A,298}$	$\Delta H^{\circ}_{A,298}$	$\Delta S^{\circ}_{A,298}$	ΔC_{pA}	$\Delta H^{\ddagger}(\Lambda)$	ref
Acetonitrile (ε = 35.96; $\Delta H^{\ddagger}(\eta)$ = 4.73 ± 0.01 kJ mol^{-1})						
[emim][BF_4]	−6.9 ± 0.6	4.2 ± 0.3	37.3 ± 1.0		6.22 ± 0.02	c
[emim][BF_4]	−7.2 ± 0.5	3.8 ± 0.2	36.7 ± 0.8	47 ± 28	6.17 ± 0.02	38
[emim][$EtSO_4$]	−9.21 ± 0.01	1.55 ± 0.06	36.1 ± 0.2	39 ± 8	6.38 ± 0.02	17
[bmim][BF_4]	−6.8 ± 0.5	3.7 ± 0.2	35.3 ± 0.8		6.24 ± 0.01	c
[bmim][BF_4]	−7.2 ± 0.2	3.8 ± 0.1	37.0 ± 0.4		6.19 ± 0.03	38
[bmim][PF_6]	−6.8 ± 0.2	1.93 ± 0.10	29.3 ± 0.3		6.22 ± 0.02	c
[bmim][Cl]	−10.3 ± 0.4	3.2 ± 0.2	45.5 ± 0.6	−20 ± 20	6.64 ± 0.02	18
[bmim][Br]	−8.3 ± 1.0	1.8 ± 0.5	34 ± 2		6.36 ± 0.05	38
[bmim][Tf]	−7.877 ± 0.003	3.409 ± 0.002	37.85 ± 0.01	23.2 ± 0.2	6.25 ± 0.03	38
[hmim][BF_4]	−6.9 ± 0.6	2.9 ± 0.3	33.1 ± 1.0	99 ± 40	6.24 ± 0.01	c
[hmim][BF_4]	−7.1 ± 0.3	3.4 ± 0.1	34.9 ± 0.4	96 ± 15	6.22 ± 0.02	38
[hmim][NTf_2]	−6.3 ± 0.4	2.4 ± 0.2	29.1 ± 0.6	79 ± 25	6.29 ± 0.01	c
Dimethyl Sulfoxide (ε = 46.52; $\Delta H^{\ddagger}(\eta)$ = 11.76 ± 0.12 kJ mol^{-1})						
[bmim][BF_4]	−3.8 ± 3.8	14.5 ± 2.0	61 ± 7	−720 ± 200	13.37 ± 0.15	16
[bmim][Cl]	−6.5 ± 1.8	1.9 ± 0.9	28 ± 3		13.97 ± 0.15	16
Methanol (ε = 32.63; $\Delta H^{\ddagger}(\eta)$ = 7.776 ± 0.005 kJ mol^{-1})						
[bmim][BF_4]	−9.0 ± 0.3	2.79 ± 0.14	39.5 ± 0.5	−50 ± 24	8.85 ± 0.02	16
[bmim][Cl]	−6.8 ± 1.0	5.7 ± 0.5	42 ± 2	960 ± 60	9.27 ± 0.02	16
Water (ε = 78.35; $\Delta H^{\ddagger}(\eta)$ = 15.0 ± 0.3 kJ mol^{-1})						
[bmim][$EtSO_4$][d]					16.6 ± 0.3	17
[bmim][Cl]	−4.3 ± 0.6	−10.7 ± 0.3	−21.3 ± 1.1	−480 ± 60	15.8 ± 0.3	18

[a]Calculated from $\Delta H^{\circ}_{A,298}$ and $\Delta S^{\circ}_{A,298}$. [b]Units: $\Delta G^{\circ}_{A,298}$, $\Delta H^{\circ}_{A,298}$, and $\Delta H^{\ddagger}(\Lambda)$, kJ·mol^{-1}; $\Delta S^{\circ}_{A,298}$, J·K^{-1}·mol^{-1}; ΔC_{pA}, J·K^{-1}·mol^{-1}. [c]This work. [d]Negligible association.

where $\Delta H^{\circ}_{A,298}$ and $\Delta S^{\circ}_{A,298}$ are, respectively, the standard enthalpy and entropy changes for the ion association process at 298.15 K. The corresponding heat capacity change, ΔC_{pA}, will obviously only be relevant if $\Delta G^{\circ}_{A}(T)$ shows a notable curvature. Note that in eq 11 T^* = 298.15 K and ΔC_{pA} are assumed to be independent of temperature. The obtained parameters are summarized in Table 2 together with literature results.

The main finding of Table 2 is that for AN $\Delta H^{\circ}_{A,298}$ and $\Delta S^{\circ}_{A,298}$ are positive. Thus, ion association of imidazolium ILs is entropy driven in this solvent. Apparently, anion−cation attractions through Coulomb and van der Waals forces (and possibly weak hydrogen bonds[43]) are not sufficient in themselves to promote ion-pair formation. Since the dielectric data for the imidazolium tetrafluoroborates, [bmim][Cl] and [hmim][NTf_2], indicated that only the imidazolium moiety is solvated, this suggests that the main contribution to $\Delta S^{\circ}_{A,298}$ arises from the release of cation-solvating AN molecules. Such a view is supported by the rather similar entropy values, ∼35 J·K^{-1}·mol^{-1}, for most IL + AN systems of Table 2. The larger value for [bmim][Cl] might be due to the rather diffuse location of the anion in the ion pair. At least Car−Parrinello simulations for [emim][Cl] in water suggest that.[44] The smaller value of $\Delta S^{\circ}_{A,298}$ for [hmim][NTf_2] might be related to the preference for the anion's cis conformer in the CIP, Figure 5, but obviously such an argument does not apply to [bmim][PF_6].

Values for $\Delta H^{\circ}_{A,298}$ in AN range from 1.8 to 4.2 kJ·mol^{-1}, Table 2. For the given series the association enthalpy seems to depend mainly on the nature of the anion but not of the cation, suggesting that the cation's imidazolium ring is essential for cation−anion interactions. However, Coulomb attractions between the charges of anion and cation are clearly not the only factor affecting $\Delta H^{\circ}_{A,298}$. The smallest (least unfavorable) value was found for [emim][$EtSO_4$]. Probably, this results from strong dipole−dipole interactions between anions ($\mu_{eff} \approx 14.0$ D) and cations ($\mu_{eff} \approx 4.5$ D) as such were found for this IL in dichloromethane.[34] This explanation may also apply to [hmim][NTf_2] as the dipole moment of the anion's cis conformer is pretty large (μ_{eff}(cis) = 5.3 D) but fails for [bmim][Tf] as $\Delta H^{\circ}_{A,298}$ is similar to values for the tetrafluoroborates despite $\mu_{eff}(Tf^-) \approx 3.6$ D.[47] On the other hand, the spherical anions ($\mu_{eff,-} = 0$) exhibit a nice correlation of $\Delta H^{\circ}_{A,298}$ with anion polarizability, Figure 8, suggesting a marked contribution from dispersive interactions to anion−cation attraction. This is in line with findings of Zahn et al.[48]

The database for the other solvents listed in Table 2 is too meagre for a meaningful discussion since, except for [bmim][Cl] + water,[18] no independent information on ion solvation and on the nature of the formed ion-pair species is available. Nevertheless, it appears that in dimethyl sulfoxide and methanol ion association is also entropy driven and probably accompanied by ion desolvation. On the other hand, ion pairing in water is weak, as expected, but apparently enthalpy driven for the only example with $K^{\circ}_{A}(T)$ values so far, [bmim][Cl].[18] Almost certainly, this is due to the specific hydration pattern of the formed contact ion pair.[44] The available data for ΔC_{pA} is too patchy for a meaningful discussion.

Ion Transport. $\Lambda^{\infty}(=\lambda^{\infty}_{+} + \lambda^{\infty}_{-}$ for 1:1 electrolytes with limiting single-ion conductivities, λ^{∞}_{+} and λ^{∞}_{-}, of cation and anion) informs on ion mobility in the absence of solute−solute interactions and is thus indicative for ion−solvent interactions.[10,11] This is even more the case for the constituting λ^{∞}_{i} ($i = +, -$) values as these can be directly linked to the (mutual) diffusion coefficients of the ions and used to calculate effective hydrodynamic (Stokes) radii. As independently determined diffusion coefficients are lacking and the interpretation of Stokes radii in terms of ion solvation is questionable,[49] we limit here discussion to single-ion conductivities.

dx.doi.org/10.1021/jp412344a | J. Phys. Chem. B XXXX, XXX, XXX−XXX

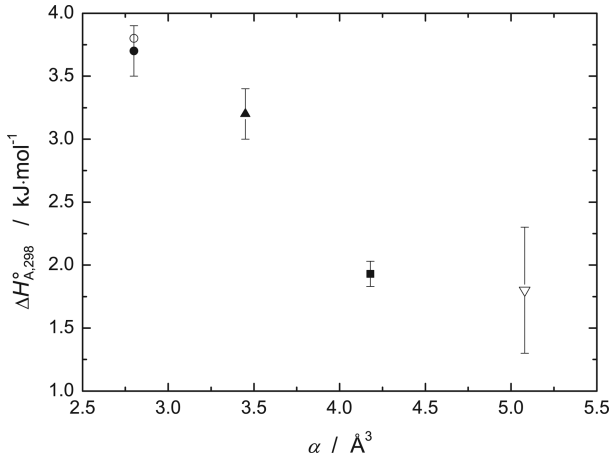

Figure 8. Standard enthalpy of ion association, $\Delta H^{\circ}_{A,298}$, as a function of anion polarizability, α, for [bmim][X] ILs in AN for $X^- = BF_4^-$ (this work, black filled circles; ref 38, black open circles), Cl^- (black filled up-triangles),[15] PF_6^- (black filled boxes, this work), and Br^- (black open down-triangles).[38] Except for Br^-,[42] anion polarizabilities were taken from Bica et al.[46]

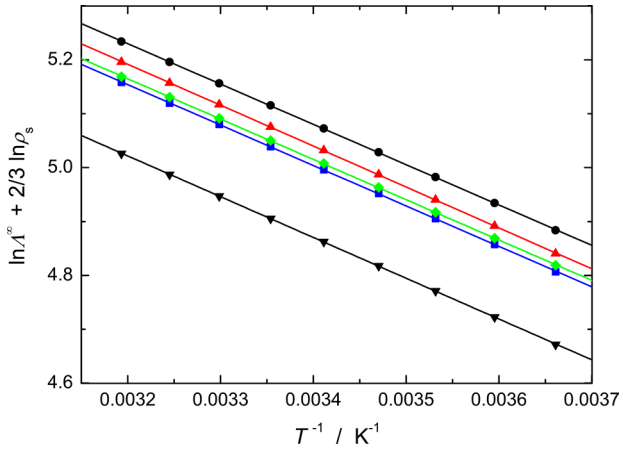

Figure 9. Brummer–Hills plot,[54] $\ln \Lambda^{\infty} + (2/3) \ln \rho_s$, as a function of T^{-1}, for ILs in AN: [emim][BF_4] (black filled circles), [bmim][BF_4] (red filled up-triangles), [bmim][PF_6] (green filled diamonds), [hmim][BF_4] (blue filled boxes), and [hmim][NTf_2] (black filled down-triangles).

In order to split Λ^{∞}, reference data tracing back to anchor values determined from transference numbers have to be known for one of the λ_i^{∞}.[11] In their critical data compilation Barthel and Neueder[23] recommended for AN solutions at 298.15 K the values of $\lambda_-^{\infty}(Cl^-) = 92.36\ \Omega^{-1}\cdot cm^2\cdot mol^{-1}$, $\lambda_-^{\infty}(BF_4^-) = 107.48\ \Omega^{-1}\cdot cm^2\cdot mol^{-1}$, and $\lambda_-^{\infty}(PF_6^-) = 103.09\ \Omega^{-1}\cdot cm^2\cdot mol^{-1}$. With the corresponding Λ^{∞} of Table 1 this yielded for the limiting single-ion conductivity of $[bmim]^+$ values of $\lambda_+^{\infty}([bmim]^+)$ = 81.55,[18] 81.81, and 81.61 $\Omega^{-1}\cdot cm^2\cdot mol^{-1}$, which are in excellent agreement with each other. Thus, significant systematic errors in the used reference data or our measurements can be excluded. For the other studied imidazolium cations $\lambda_-^{\infty}([emim]^+) = 89.62\ \Omega^{-1}\cdot cm^2\cdot mol^{-1}$ and $\lambda_-^{\infty}([hmim]^+) = 75.17\ \Omega^{-1}\cdot cm^2\cdot mol^{-1}$ were obtained and from the latter $\lambda_-^{\infty}([NTf_2]^-) = 84.65\ \Omega^{-1}\cdot cm^2\cdot mol^{-1}$ was calculated. A rather general observation for pure imidazolium ILs is that the cation diffuses faster than the anion despite the eventually smaller size of the latter.[50−53] As reflected by the corresponding λ_i^{∞} values, this is not the case anymore for dilute solutions of the ILs in AN. Here the smaller anions, Cl^-, BF_4^-, and PF_6^-, are considerably faster than the smallest cation, $[emim]^+$. Only the big $[NTf_2]^-$ anion has a mobility comparable to the cations.

Except for values reported by Kalugin et al.[38] for BF_4^-, appropriate reference data for other temperatures are apparently not available. Unfortunately, the value given in ref 38 for $\lambda_i^{\infty}(BF_4^-)$ at 298.15 K (115.4 $\Omega^{-1}\cdot cm^2\cdot mol^{-1}$) exceeds the recommendation of Barthel and Neueder[23] by 7%, and derived cation data are correspondingly smaller than ours. We therefore abstain from calculating $\lambda_i^{\infty}(emim^+)$, $\lambda_i^{\infty}(emim^+)$, $\lambda_-(hmim^+)$, and $\lambda_i^{\infty}(NTf_2^-)$ at other temperatures.

Charge transport in electrolyte solutions can be viewed as a succession of random jumps of the ions, limited by an average activation barrier.[54] The associated Eyring activation enthalpy for charge transport, $\Delta H^{\ddagger}$, which is the transference-number weighted average of the corresponding $\Delta H^{\ddagger}$ values of the constituent ions, can be determined[54] as the slope of Λ^{∞} vs T.

$$\ln \Lambda^{\infty} + \frac{2}{3} \ln d_s = -\frac{\Delta H^{\ddagger}(\Lambda^{\infty})}{RT} + B \qquad (12)$$

where B is an empirical constant (Figure 9). In essence, $\Delta H^{\ddagger}(\Lambda^{\infty})$ is determined by the size of the ions and the strength of ion–solvent interactions. Note that ion–ion interactions, i.e., effects related to ion pairing, do not contribute as the infinite-dilution limit is considered. On the other hand, $\Delta H^{\ddagger}(\Lambda^{\infty})$ can be compared to the activation enthalpy of viscous flow of the pure solvent, $\Delta H^{\ddagger}(\eta)$, for which the size and shape of the solvent molecules as well as their mutual interactions are determining.

For the IL + solvent mixtures of this investigation plots of Λ^{∞} vs T are linear and essentially parallel, Figure 9. A perusal of Table 2 reveals that $\Delta H^{\ddagger}(\Lambda^{\infty})$ does not vary much with the IL but strongly depends on the solvent. In all cases $\Delta H^{\ddagger}(\Lambda^{\infty}) > \Delta H^{\ddagger}(\eta)$ but whereas for aqueous solutions the activation enthalpy of conductivity exceeds that of viscosity by only ~8%, the difference is ~16% for methanol and dimethyl sulfoxide and even ~30% for acetonitrile. Keeping in mind that the cation's imidazolium ring is solvated by AN molecules (Figure 4) which are slowed in their rotational dynamics by a factor of ~8–10 compared to bulk AN, whereas the retardation factor of water molecules surrounding hydrophobic solutes is only ~1.5–3,[15,26,55] it appears that the rate of solvent-shell rearrangement and associated solvent exchange with the bulk affect the ratio $\Delta H^{\ddagger}(\Lambda^{\infty})/\Delta H^{\ddagger}(\eta)$.

CONCLUDING REMARKS

Dielectric spectroscopy can yield detailed information on solvation and ion-association processes in solutions, such as the nature and concentration of formed ion pairs, effective solvation numbers, and the associated cooperative dynamics of solvent and solute.[15] However, the spectra are often rather featureless due to strong band overlap. While formal description of such data is almost always possible, the assignment and interpretation of the resolved bands may be problematic. Therefore, as for all other techniques, inference from dielectric spectroscopy not only has to be self-consistent in its conclusions but requires backup by independent information.

The present spectra of [hmim][NTf_2] + AN are a good example. From their variation with IL mole fraction (Supporting Information Figure S1) the presence of—at least—two modes was obvious. Indeed, the fit of all mixture spectra with the CC+D model, eq 3, not only yielded the best fit in most cases but also a smooth set of parameters (Supporting Information Table S4).

dx.doi.org/10.1021/jp412344a | J. Phys. Chem. B XXXX, XXX, XXX–XXX

This was not the case for other tried fit models. However, from the shape of the pure-component spectra and the variation of relaxation times (Supporting Information Figure S2) and amplitudes (Figure 3) with IL mole fraction it was obvious that both resolved modes were composites. The higher frequency Debye (D) mode was obviously dominated by AN at $x \lesssim 0.5$ (Figure 3b). Thus, the marked difference, ΔS_{AN}, between expected and detected amplitude was clear evidence for ion solvation. The obtained effective solvation numbers, Z, for [hmim][NTf_2], together with those for the previously studied tetrafluoroborates[7] and [bmim][Cl][18] revealed that in these mixtures Z does neither depend on the anion nor on the length of the cation's alkyl chain (Figure 4) and thus monitors the interactions of the imidazolium ring with the surrounding AN molecules. This is in line with qualitative information from MD simulations and vibrational spectroscopy.[24,32]

Interpretation of the lower frequency Cole−Cole (CC) relaxation was far less straightforward. Clearly, the assumption of only $[bmim]^+$ cations as the relaxing species was insufficient (Figure 3a). There was also evidence for the presence of ion pairs at low IL content (Figure 3 of ref 19 and Supporting Information Figure S5). However, evaluation of the amplitude, S_1, required information on the ion-pair dipole moment and thus on the possible species, i.e., contact or solvent-shared ion pair. Additionally, there were hints that the dynamics of solvating AN molecules was on a time scale similar to the reorientation of $[bmim]^+$ and its ion pair.[7] Based on DRS data alone, this left options for the extrapolated standard-state association constant ranging from $K_A^\circ \approx 500\ M^{-1}$ for the assumption that mode 1 was only due to CIPs and free cations to $K_A^\circ \approx 1\ M^{-1}$ if solvent-shared ion pairs, free $[bmim]^+$, *and* solvating AN were contributing. With the anchor value of $K_A^\circ = 12.67\ M^{-1}$ for [bmim][NTF_2] from dilute-solution conductivity measurements, the only option left for the assignment of the CC mode was the simultaneous presence of contact ion pairs, free $[bmim]^+$, and solvating AN molecules.

The dilute-solution conductivity measurements not only showed that imidazolium ILs are only moderately associated in AN and thus comparable to common organic electrolytes. The temperature dependence of K_A° revealed that their ion pairing is entropy driven and thus linked to cation desolvation, in line with the only moderate strength (solvent retardation factor ~10−20) of cation−AN interactions. This appears to be also the case for other organic solvents but not for water where the much smaller retardation factor (~1.3−3) indicates easy replacement of solvating H_2O by the counterion. Comparison of the activation energies of conductivity, $\Delta H^{\ddagger}(\Lambda^\infty)$, and viscous flow, $\Delta H^{\ddagger}(\eta)$, corroborates this view. Unfortunately, limiting single-ion conductivities, λ_i^∞, could only be determined at 298.15 K so that the associated activation energies are not accessible but based on the inference from DRS the sequence $\Delta H^{\ddagger}(\lambda_+^\infty) > \Delta H^{\ddagger}(\Lambda^\infty) > \Delta H^{\ddagger}(\lambda_-^\infty) \approx \Delta H^{\ddagger}(\eta)$ is expected for imidazolium ILs in AN.

■ ASSOCIATED CONTENT

Supporting Information

Tables with conductivity data, solvent properties, and relaxation parameters and additional figures illustrating dielectric loss, relaxation times of the lower frequency CC mode and the higher frequency D mode, width pamameter of the lower frequency CC mode, molar conductivity and excess volume as a function RTIL mole fraction of [hmim][BF_4], and effective dipole moment and ion-pair concentrations of [hmim][BF_4]. This material is available free of charge via the Internet at http://pubs.acs.org.

■ AUTHOR INFORMATION

Corresponding Authors

*E-mail: Marija.Bester@fkkt.uni-lj.si.

*E-mail: Richard.Buchner@chemie.uni-regensburg.de.

Notes

The authors declare no competing financial interest.

■ ACKNOWLEDGMENTS

The authors gratefully acknowledge financial support by the Slovenian Research Agency (Grant P1-0201) and COST Actions CM1206 for M.B.-R. and by the Deutsche Forschungsgemeinschaft for A.S. and R.B. within the framework of Priority Program SPP 1191, "Ionic Liquids".

■ REFERENCES

(1) Plechkova, N. V., Rogers, R. D., Seddon, K. R., Eds. *Ionic Liquids: From Knowledge to Application*; ACS Symposium Series 1030; American Chemical Society: Washington, DC, USA, 2009.

(2) Weingärtner, H. Understanding Ionic Liquids at the Molecular Level: Facts, Problems and Controversies. *Angew. Chem., Int. Ed.* **2008**, *47*, 654−670.

(3) Ueno, K.; Tokuda, H.; Watanabe, M. Ionicity in ionic liquids: correlation with ionic structure and physicochemical properties. *Phys. Chem. Chem. Phys.* **2010**, *12*, 1649−1658.

(4) Castner, E. W.; Wishart, F. Spotlight on Ionic Liquids. *J. Chem. Phys.* **2010**, *132*, 120901.

(5) Angell, C. A.; Ansari, Y.; Zhao, Z. Ionic Liquids: Past, present and future. *Faraday Discuss.* **2012**, *154*, 9−27.

(6) Chaban, V. V.; Prezhdo, O. V. Ionic and Molecular Liquids: Working Together for Robust Engineering. *J. Phys. Chem. Lett.* **2013**, *4*, 1423−1431.

(7) Stoppa, A.; Hunger, J.; Hefter, G.; Buchner, R. Structure and Dynamics of 1-*N*-Alkyl-3-*N*-Methylimidazolium Tetrafluoroborate + Acetonitrile Mixtures. *J. Phys. Chem. B* **2012**, *116*, 7509−7521.

(8) Chaban, V. V.; Voroshylova, I. V.; Kalugin, O. N.; Prezhdo, O. V. Acetonitrile Boosts Conductivity of Imidazolium Ionic and Molecular Liquids. *J. Phys. Chem. B* **2012**, *116*, 7719−7727.

(9) Borodin, O.; Henderson, W. A.; Fox, E. T.; Berman, M.; Gobet, M.; Greenbaum, S. Influence of Solvent on Ion Aggregation and Transport in PY_{15}TFSI Ionic Liquid-Aprotic Solvent Mixtures. *J. Phys. Chem. B* **2013**, *117*, 10581−10588.

(10) Barthel, J. M. G.; Krienke, H.; Kunz, W. *Physical Chemistry of Electrolyte Solutions-Modern Aspects* ; Steinkopff and Springer: Darmstadt, Germany, and New York, NY, USA, 1998.

(11) Bockris, J. O.; Reddy, A. K. N. *Modern Electrochemistry*, 2nd ed.; Plenum: New York, 1998; Vol. *1*.

(12) Strictly speaking, eq 1 requires activities, $a_i = c_i y_i$, instead of concentrations; see eq 6. However, as activity coefficients $y_i \rightarrow 1$ for $c \rightarrow 0$ and DRS determines ion-pair concentrations, c_{IP}, at finite c, this representation is preferred here.

(13) Marcus, Y.; Hefter, G. Ion Pairing. *Chem. Rev.* **2006**, *106*, 4585−4621.

(14) Hefter, G. When spectroscopy fails: The measurement of ion pairing. *Pure Appl. Chem.* **2006**, *78*, 1571−1586.

(15) Buchner, R.; Hefter, G. Interactions and Dynamics in Electrolyte Solutions by Dielectric Spectroscopy. *Phys. Chem. Chem. Phys.* **2009**, *11*, 8954−8999.

(16) Bešter-Rogač, M.; Hunger, J.; Stoppa, A.; Buchner, R. Molar conductivities and association constants of [bmim][Cl] and [bmim]-[BF_4] in methanol and DMSO. *J. Chem. Eng. Data* **2010**, *55*, 1799−1803.

(17) Bešter-Rogač, M.; Hunger, J.; Stoppa, A.; Buchner, R. l-Ethyl-3-methylimidazolium Ethylsulfate in Water, Acetonitrile and Dichloromethane: Molar Conductivities and Association Constants. *J. Chem. Eng. Data* **2011**, *56*, 1261−1267.

(18) Bešter-Rogač, M.; Stoppa, A.; Hunger, J.; Hefter, G.; Buchner, R. Association of Ionic Liquids in Solution: A Combined Dielectric and

Conductivity Study of [bmim][Cl] in Water and in Acetonitrile. *Phys. Chem. Chem. Phys.* **2011**, *13*, 17588−17598.
(19) Lohse, P. N.; Bartels, N.; Stoppa, A.; Buchner, R.; Lenzer, T.; Oum, K. Spectroscopy and Dynamics of $[C_6mim]$ + $[Tf_2N]^-$ Acetonitrile Mixtures. *Phys. Chem. Chem. Phys.* **2012**, *14*, 3596−3603.
(20) Stoppa, A.; Hunger, J.; Buchner, R. Conductivities of binary mixtures of ionic liquids with polar solvents. *J. Chem. Eng. Data* **2009**, *54*, 472−479.
(21) Bešter-Rogač, M.; Habe, D. Modern advances in electrical conductivity measurements of solutions. *Acta Chim. Slov.* **2006**, *53*, 391−395.
(22) Lide, D. R., Ed. *CRC Handbook of Chemistry and Physics*, 85th ed.; CRC Press: Boca Raton, FL, USA, 2004.
(23) Barthel, J.; Neueder, R. In *Chemistry Data Series*; Eckermann, R., Kreysa, C., Eds.; DECHEMA Monographien; DECHEMA: Frankfurt, Germany, 1996; Vol. *XII*.
(24) Bardak, F.; Xiao, D.; Hines, L. G.; Son, P.; Bartsch, R. A.; Quitevis, E. L.; Yang, P.; Voth, G. A. Nanostructural organization of acetonitrile/ionic liquid mixtures: Molecular dynamics simulations and optical Kerr effect spectroscopy. *ChemPhysChem* **2012**, *13*, 1687−1700.
(25) Sonnleitner, T.; Nikitina, V.; Nazet, A.; Buchner, R. Do H-Bonds Explain Strong Ion Aggregation in Ethylammonium Nitrate + Acetonitrile Mixtures? *Phys. Chem. Chem. Phys.* **2013**, *15*, 18445−18452.
(26) Rahman, H. M. A.; Hefter, G.; Buchner, R. Hydrophilic and Hydrophobic Hydration of Sodium Propanoate and Sodium Butanoate in Aqueous Solution. *J. Phys. Chem. B* **2013**, *117*, 2142−2152.
(27) In contrast to the well known Kirkwood correlation factor, g_K, which describes dipole−dipole correlations in neat dipolar fluids and which can be derived from statistical mechanics,[56] the present g_j values may also incorporate cross-correlations among different dipolar species in the mixture.[34]
(28) Tsuzuki, S.; Tokuda, H.; Hayamizu, K.; Watanabe, M. Magnitude and Directionality of Interaction in Ion Pairs of Ionic Liquids: Relationship with Ionic Conductivity. *J. Phys. Chem. B* **2005**, *109*, 16474−16481.
(29) Zhao, W.; Leroy, F.; Heggen, B.; Zahn, S.; Kirchner, B.; Balasubramanian, S.; Müller-Plathe, F. Are there stable ion-pairs in room-temperature ionic liquids? Molecular dynamics simulations of l-*n*-butyl-3-methylimidazolium hexafluorophosphate. *J. Am. Chem. Soc.* **2009**, *131*, 15825−15833.
(30) From semiempirical calculations using MOPAC2009[31] and the PM6 Hamiltonian on [bmim][BF_4]. The cation radius, a_+, was assumed to be the difference between the calulated distance d([bmim][BF_4]) = 0.365 nm (corresponding to a configuration where the anion is sitting over the imidazolium ring of the cation) and the anion radius, a_-, reported for BF_4^-.[10] However, variation of a_+ within reasonable limits had only minor influence on the obtained K_A°.
(31) Stewart, J. J. P. *MOPAC2009, Stewart Computational*; CAChe Research: Beaverton, OR, USA, 2009
(32) Zheng, Y.-Z.; Wang, N.-N.; Luo, J.-J.; Yu, Z.-W. Hydrogen-bonding interactions between [bmim] [BF_4] and acetonitrile. *Phys. Chem. Chem. Phys.* **2013**, *15*, 18055−18064.
(33) Hunger, J.; Stoppa, A.; Buchner, R.; Hefter, G. From Ionic Liquid to Electrolyte Solution: Dynamics of Binary l-*N*-Butyl-3-*N*-methyl-imidazolium Tetrafluoroborate + Dichloromethane Mixtures. *J. Phys. Chem. B* **2008**, *112*, 12913−12919.
(34) Hunger, J.; Stoppa, A.; Buchner, R.; Hefter, G. Dipole Correlations in the Ionic Liquid l-*N*-Ethyl-3-*N*-methylimidazolium Ethylsulfate and Its Binary Mixtures with Dichloromethane. *J. Phys. Chem. B* **2009**, *113*, 9527−9537.
(35) The minimum for μ_{eff} at $x \approx 0.05$ (Figure S5 of the Supporting Information) is almost certainly an artefact of the polynomial fits to S_1 and S_2 that propagates to K_A (Figure 6) and c_{IP} (Figure S6 of the Supporting Information).
(36) Hunger, J.; Stoppa, A.; Schrodle, S.; Hefter, G.; Buchner, R. Temperature dependence of the dielectric properties and dynamics of ionic liquids. *ChemPhysChem* **2009**, *10*, 723−733.
(37) Canongia Lopes, J. N.; Shimizu, K.; Pádua, A. A. H.; Umebayashi, Y.; Fukuda, S.; Fuji, K.; Ishiguro, S. A Tale of Two Ions: The Conformational Landscapes of Bis(trifluoromethanesulfonyl)amide and *N*,*N*-Dialkylpyrrolidinium. *J. Phys. Chem. B* **2008**, *112*, 1465−1472.
(38) Kalugin, O. N.; Voroshylova, I. V.; Riabchunova, A. V.; Lukinova, E. V.; Chaban, V. V. Conductimetric study of binary systems based on ionic liquids and acetonitrile in a wide concentration range. *Electrochim. Acta* **2013**, *105*, 188−199.
(39) The present findings show that, in ref 7, the use of ion-pair dipole moments obtained from extrapolating $\mu_{IP,eff}$ (x) to $x = 0$ is the main reason for the differenee in K_A° from DRS and conductivity measurements.
(40) Fox, E. T.; Paillard, E.; Borodin, O.; Henderson, W. A. Physicochemical Properties of Binary Ionic Liquid-Aprotic Solvent Electrolyte Mixtures. *J. Phys. Chem. C* **2013**, *117*, 78−84.
(41) Barthel, J.; Iberl, L.; Rossmaier, J.; Gores, H. J.; Kaukal, B. Conductance of 1,1-Electrolytes in Acetonitrile Solutions From −40 to 35 °C. *J. Solution Chem.* **1990**, *19*, 321−337.
(42) Wang, H.; Wang, J.; Zhang, S.; Pei, Y.; Zhuo, K. Ion Association of the Ionic Liquids $[C_4mim][BF_4]$, $[C_4mim][PF_6]$, and $[C_nmim]$Br in Molecular Solvents. *ChemPhysChem* **2009**, *10*, 2516−2523.
(43) Fumino, K.; Wulf, A.; Ludwig, R. The potential role of hydrogen bonding in aprotic and protic ionic liquids. *Phys. Chem. Chem. Phys.* **2009**, *11*, 8790−8794.
(44) Spickermann, C.; Thar, J.; Lehmann, S. B. C; Zahn, S.; Hunger, J.; Buchner, R.; Hunt, P. A.; Welton, T.; Kirchner, B. Why are ionic liquids mainly associated in water? A Car-Parinello study of l-ethyl-3-methyl-imidazolium chloride water mixture. *J. Chem. Phys.* **2008**, *129*, 104505.
(45) Marcus, Y. *Ion Properties*; Wiley: Chichester, U.K., 1997.
(46) Bica, K.; Deetlefs, M.; Schröder, C.; Seddon, K. R. Polarisabilities of alkylimidazolium ionic liquids. *Phys. Chem. Chem. Phys.* **2013**, *15*, 2703−2711.
(47) Placzek, A.; Hefter, G.; Rahman, H. M. A.; Buchner, R. Dielectric Relaxation Study of the Ion Solvation and Association of $NaCF_3SO_3$, $Mg(CF_3SO_3)_2$ and $Ba(ClO_4)_2$ in *N*,*N*-Dimethylformamide. *J. Phys. Chem. B* **2011**, *115*, 2234−2242.
(48) Zahn, S.; Uhlig, F.; Thar, J.; Spickermann, C.; Kirchner, B. Intermolecular Forces in an Ionic Liquid ([Mim][CI]) versus Those in a Typical Salt (NaCl). *Angew. Chem., Int. Ed.* **2008**, *47*, 3639−3641.
(49) Marcus, Y. Are Ionic Stokes Radii of Any Use? *J. Solution Chem.* **2012**, *41*, 2082−2090.
(50) Harris, K. R.; Kanakubo, M.; Tsuchihashi, N.; Ibuki, K.; Ueno, M. Effect of Pressure on the Transport Properties of Ionic Liquids: l-Alkyl-3-methylimidazolium Salts. *J. Phys. Chem. B* **2008**, *112*, 9830−9840.
(51) Tsuzuki, S.; Shinoda, W.; Saito, H.; Mikami, M.; Tokuda, H.; Watanabe, M. Molecular Dynamics Simulations of Ionic Liquids: Cation and Anion Dependence of Self-Diffusion Coefficients of Ions. *J. Phys. Chem. B* **2009**, *113*, 10641−10649.
(52) Tsuzuki, S. Factors Controlling the Diffusion of Ions in Ionic Liquids. *ChemPhysChem* **2012**, *13*, 1664−1670.
(53) Hayamizu, K.; Tsuzuki, S.; Seki, S.; Umebayashi, Y.; Multinuclear, N. M. R. Studies on Translational and Rotational Motion for Two Ionic Liquids Composed of BF_4 Anion. *J. Phys. Chem. B* **2012**, *116*, 11284−11291.
(54) (a) Brummer, S. B.; Hills, G. J. Kinetics of ionic conductance. Part 1.—Energies of activation and the constant volume principle. *Trans. Faraday Soc.* **1961**, *57*, 1816−1822. (b) Brummer, S. B.; Hills, G. J. Kinetics of ionic conductance. Part 2.—Temperature and pressure coefficients of conductance. *Trans. Faraday Soc.* **1961**, *57*, 1823−1837.
(55) Laage, D.; Stirneman, G.; Sterpone, F.; Rev, R.; Hynes, J. T. Reorientation and Allied Dynamics in Water and Aqueous Solutions. *Annu. Rev. Phys. Chem.* **2011**, *62*, 395−416.
(56) (a) Böttcher, C. F. J., Ed. *Theory of Electric Polarization*, Vol. *1*; Elsevier: Amsterdam, 1973. (b) Böttcher, C. F. J., Bordewijk, P., Eds. *Theory of Electric Polarization*, Vol. *2*; Elsevier: Amsterdam, 1978.